Desalination and Water Treatment
www.deswater.com
29 (2011) 218–226
May
1944-3994 / 1944-3986
doi: 10.5004/dwt.2011.2099

Removal of cadmium from simulated wastewaters by electrodeposition on stainless steeel tubes bundle electrode

Abbas Hamid Sulaymon[a], Adel Obaid Sharif[b], Thana Kamil Al-Shalchi[c]*

[a]*Environmental Engineering Department, University of Baghdad, Iraq*
[b]*Faculty of Engineering and Physical Sciences, University of Surrey, UK*
[c]*Environmental Engineering Department, University of Baghdad, Iraq*
Tel. +964 7901 320849; email: talshalchi@yahoo.com

Received 22 June 2010; Accepted in revised form 9 December 2010

ABSTRACT

Electrochemical processes can provide valuable contributions to the protection of the environment through implementation of effluent treatment and production-integrated processes for the minimization of waste and toxic compounds. The performance of a novel pilot scale, fixed bed flow-through cell, consisting of stainless steel tubes bundle cathode, in the removal of cadmium was investigated in the batch re-circulation mode; utilizing the potential results obtained from rotating disc electrode experiments in batch mode. The studied electrochemical reaction was the cathodic reduction of Cd^{2+} using 0.5 M sodium sulphate as supporting electrolyte. The analyzed parameters were different electrolyte pH, different initial Cd^{2+} concentrations, and different Reynolds numbers. The tubes bundle consisted of 920 tubes of 0.6 cm outer diameters. The overall empirical mass transfer correlation was found to be: $Sh = 0.51\ Re^{0.859}\ Sc^{1/3}$ for $5 < Re < 20$ and $Sc = 649$. Experimental results, analysis and correlations showed good performance of the cell and proved its adequacy in the removal of Cd^{2+} from simulated effluents.

Keywords: Electrochemical; Fixed bed flow through cell; Cadmium; Tubes bundle electrode

1. Introduction

With a rapidly growing world population and an increasing number of reports on detrimental effects on the environment, its protection has become a major issue and a crucial factor for future technological progress, which will have to meet the requirements for sustainable development. The strategies for environmental protection in industry generally include processes or products which have no or less harmful effects on the environment. Electrochemistry has important roles to play in these strategies; industrial electrochemistry has undergone developments towards cleaner processes and more environmentally friendly products [1].

Cadmium is a toxic and bio-persistent element and, once absorbed by an organism, remains resident for many years although it is eventually excreted. In humans, long-term exposure is associated with renal dysfunctions. High exposure can lead to obstructive lung disease and has been linked to lung cancer [2].

Waste streams containing low concentrations of cadmium are produced from processes such as cadmium electroplating, zinc electrowinning, metal-pickling processes and recycling of waste batteries. The legal limitations concerning cadmium discharge in effluents are very stringent due to the highly toxic nature of cadmium salts,

* Corresponding author.

which necessitates the development of technologies that may prevent or correct the deleterious effect of cadmium ions [3].

The electrolytic method for the removal of heavy metals from aqueous media by using porous electrodes of various geometric shapes and materials, with flowing solutions, represents a successful reactor which presents high mass-transfer conditions [4].

The batch-recycle system may be modeled satisfactorily as a simple batch reactor and there is no need to use a batch-recycle model [5]. In a simple batch electrolytic reactor, with a constant volume of electrolyte V_T, the reactant will decay from initial concentration c_o to a value $c(t)$ at time t. The rate of change of the reactant concentration is:

$$\frac{dc(t)}{dt} = -kc(t) \tag{1}$$

It can be assumed that the reaction displays first-order kinetics with respect to the reactant. A mass balance in the reactor may be written by relating $dc(t)/dt$ to the cell current as follows:

$$-\frac{dc(t)}{dt} = \frac{i(t)}{nFV_T} \tag{2}$$

where $i(t)$ is the instantaneous current density at time t.

When the conditions are chosen so that the reduction of metal ion to metal is mass transport controlled over all the surface of the three dimensional cathode, the current is [6]:

$$i(t) = i_L = nFk_m Ac(t) \tag{3}$$

Substituting Eq. (2) into Eq. (3) and integrating gives:

$$c(t) = c_0 \exp\left(-\frac{k_m At}{V_T}\right) \tag{4}$$

For the electrolytic reactor using a three dimensional porous cathode, the total area of the electrode is considered to be: $A = A_e V_e$.

Substituting in Eq. (4) gives:

$$c(t) = c \exp\left(\frac{-k_m A_e V_e t}{V_T}\right) \tag{5}$$

or

$$\ln\left(c(t)/c_0\right) = -\frac{V_e k_m A_e t}{V_T} \tag{6}$$

Eqs. (5) and (6) describe the reactant concentration as a function of time of electrolysis [5].

The aim of the present research is to study the performance of a novel electrochemical reactor with stainless steel tubes bundle electrode on the removal of cadmium from simulated wastewaters. The analyzed parameters were different electrolyte pH, different initial Cd^{2+} concentrations, and different Reynolds numbers.

2. Experimental work

The performance of a novel pilot scale fixed bed electrochemical reactor, with stainless steel tubes bundle cathode was studied. Potential values over which cadmium is controlled by mass transfer, was obtained from a rotating disc electrode experiments [7], accordingly a value of –1 V was applied for the removal of cadmium from a synthetic solution in the batch re-circulation mode.

The catholyte solution used was a 0.5 M sodium sulphate, used as supporting electrolyte, with different concentrations of cadmium sulphate (50, 100, 200, 300 and 400 mg/L) [3,8–12]. The bulk pH was adjusted to a value of 4.8. The anolyte used had the same composition as the catholyte, but without the presence of cadmium.

The catholyte and anolyte Reynolds numbers used were 1.189, 2.377, 2.972, 3.566 and 4.16.

The novel pilot scale electrolytic cell used had an overall dimension of 25×25×17 cm; it was made from four Teflon discs. A silicon rubber layer of 1 mm thickness was placed between each two disks to prevent the electrolyte leakage. The main cell compartments are the cathode chamber and the anode chamber. It consisted of the following parts, as illustrated in the schematic diagram (Fig. 1).

2.1. Cathode chamber

The cathode chamber had an overall outer dimension of 25×25×12 cm, and it consisted of three sections; the first section was used for the distribution of the catholyte at the entrance of the cell. The second section was used to install the cathode on top of a fixed perforated stainless steel plate acting as a current feeder, in addition to produce a uniform catholyte flow and distribution at the cathode entrance. The novel tubes bundle (cathode) consisted of 920 tubes of 6 mm outside diameters, 4 mm inside diameters and 3 cm length, arranged in triangular pitch arrangement as seen in Fig. 2. The adoption of a stainless steel tubes bundle accomplishes many advantages:

- a total surface area of 8959.822 cm^2
- a specific surface area of 8.623 cm^{-1}
- exposed to flow from both outside and inside surfaces
- increase the electrolyte velocities inside the tubes
- stainless steel is an inert, available and non-toxic material
- the tubes are easy to clean without dismantling the cathode, by flashing with H_2SO_4.

The third section was used to collect the catholyte to the output of the cell.

2.2. Anode chamber

The Teflon anode chamber had an overall outer dimension of 25×25×5 cm, and it consisted of one disc; the

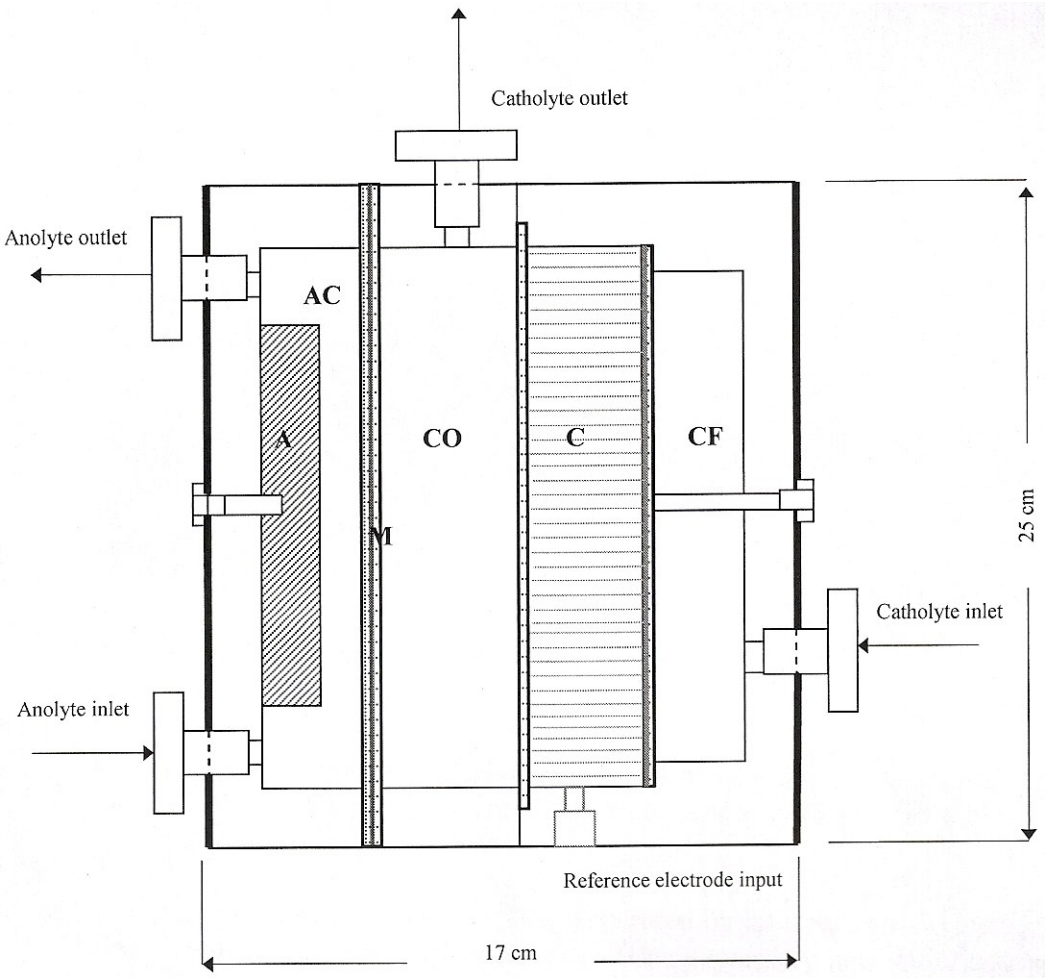

Fig. 1. Schematic diagram of the electrolytic cell. A – anode (graphite); AC – anolyte chamber; M – membrane and support plates; C – cathode (stainless steel tube bundle); CF – catholyte feeder section; CO – catholyte outlet section.

Fig. 2. The tubes bundle electrode (6 mm diameter tubes).

anode was made of a graphite disc of 14 cm diameter and 2 cm thickness.

2.3. Membrane

The anode chamber and cathode chamber were separated by an ionic ion-exchange membrane, allowing the anolyte and catholyte to flow separately and simultaneously in a closed circuit. It was made in the USA by Sybron Chemicals Inc., Brimming, N.J. Prod. No. (MA-3475).

The pilot flow system used, operating under batch re-circulating conditions, consisted in addition to the electrochemical cell, the catholyte and anolyte porcelain reservoirs, two recirculation pumps, and two sets of flow meters for measuring the catholyte and anolyte flow rates.

At time intervals of 15 min, catholyte samples were taken from the catholyte reservoir in order to be analyzed for Cd^{2+} concentrations by atomic absorption spectrometry, model Hitachi 170–50.

3. Results and discussion

The performance of a novel pilot scale, fixed bed cell, consisting of stainless steel tubes bundle cathode, in the removal of cadmium was examined in the batch recirculation mode. A potential equal to –1 V was utilized throughout the work. This potential was obtained from a rotating disc electrode experiments; it was determined from series of polarization curves, where the midpoint of the plateaus –1.0 V represents the appropriate reduction potential for the removal of Cd^{2+} from solutions. Fig. 3 illustrates an example of a polarization curve.

Polarization curves show the plateaus regions for the series of experiments conducted at different parameters. These plateaus regions represent the limiting currents as shown in Fig. 3. The mid-points of these limiting currents plateaus are proportional to the potential values for the removal of heavy metals [13].

At low currents (section A), the change in electrode potential with current is associated with the limiting rate of electron transfer across the phase boundary between the electronically conducting electrode and the ionically conducting solution. As the overpotential increases, (section B), there is a transition region in which both electron transfer and mass transport rates play a role; whereas at the limiting current region (section C), only mass transport is the rate determining and the current reaches a limiting value which is independent of voltage over a considerable range.

In practice, the current plateau is eventually interrupted since at some more negative potential, a subsequent electrode reaction, such as hydrogen evolution, takes place. It can also be seen from Fig. 3 that the limiting current increases with the increasing of the rotation rate of the rotating disc electrode. This behavior is characteristic of a mass-transfer controlled process [14].

3.1. Effect of pH

Experiments were conducted with the pilot plant flow-through cell on the removal of Cd^{2+}. The experiment's parameters adopted were, Cd^{2+} initial concentration of 200 ppm and Reynolds number of 2.972, for solutions with initial pH values of 3, 4, 4.8, 5.5.

Fig. 4 illustrates the decrease in normalized Cd^{2+} concentration $c(t)/c_o$ with time for different pH. It can be seen that the cadmium concentration decreases exponentially with the time of electrolysis. It is also seen that Cd^{2+} removal is enhanced by increasing the pH of the solution, this is attributed to the hydrogen evolution, which is the predominant cathodic reaction at low pH values; reaching a pH value where further increase has no apparent effect on the removal of Cd^{2+}, that is when the curves become almost superimposed at a pH of 4.8; this pH value represents the value for the removal of Cd^{2+} at the limiting current.

Plotting the logarithmic normalized concentration $\ln(c(t)/c_o)$ as a function of time, gives linear relationships; the slopes of the straight lines were used to estimate the mass transfer coefficients by using Eq. (6). This equation, as stated in literature, is for a batch-recycle mode electrolysis process carried out under mass transfer control [5].

Since V_e and V_T are known parameters and A_e is calculated; then k_m can be estimated from Eq. (6). Table 1 lists k_m values as a function of pH. It can be seen that the mass transfer coefficient increases with pH and becomes almost constant at pH = 4.8.

Accordingly the pH value of 4.8 was selected for solu-

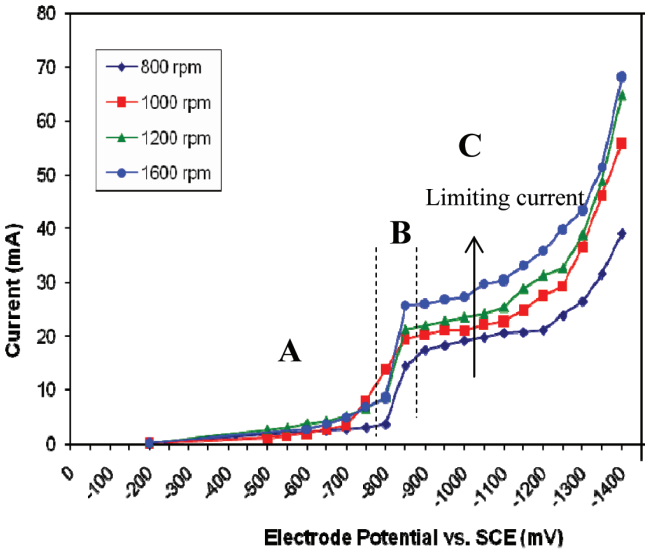

Fig. 3. Polarization curve for reduction of 100 ppm Cd^{2+}.

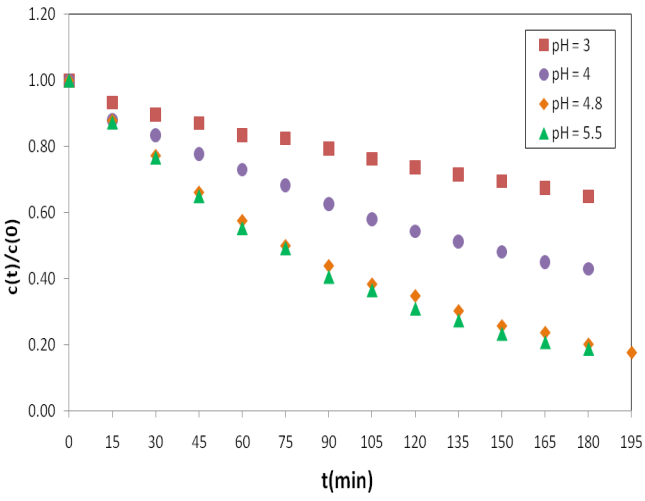

Fig. 4. Normalized concentration $c(t)/c_o$ as a function of time for different pHs, and Reynolds number of 2.972 and Cd^{2+} concentration of 200 ppm.

Table 1
Values of k_m for different pHs, and Reynolds number of 2.972 and Cd^{2+} concentration of 200 ppm

pH	$10^4\ k_m$ (cm/s)
3	0.463
4	0.917
4.8	1.657
5.5	1.778

tions for the other sets of experiments that follow. This pH is in good agreement with other researchers [11,12].

3.2. Effect of initial concentration

Experiments were carried out to study the removal rate of Cd^{2+} from solutions of different Cd^{2+} initial concentrations with catholyte and anolyte Reynolds number of 2.972.

Fig. 5 shows the curves of normalized Cd^{2+} concentration $c(t)/c_o$ as a function of time for different cadmium initial concentrations (50, 100, 200, 300, 400 ppm). As expected, cadmium concentration decays exponentially with time. It can be seen the trends and behaviors of the curves for the different Cd^{2+} concentrations are the same. Also it can be seen that a Cd^{2+} concentration of 50 ppm decays to the standard Cd^{2+} for discharge of less than 2.0 ppm; for higher concentrations, cathodes arranged in serials should be used, after re-adjusting the conditions of the electrolytes to the initial conditions.

Plotting the logarithmic normalized concentration $\ln(c(t)/c_o)$ as a function of time, gives linear relationships. Following the same previous procedures, values of k_m were calculated for each concentration.

In order to correlate the mass transfer coefficient (k_m) with the bulk concentration of Cd^{2+}, the estimated mass transfer coefficients were plotted against the logarithmic Cd^{2+} bulk concentrations, giving a linear relationship, (Fig. 6), which is expressed in the following empirical equation, with CR = 0.995:

$$k_m = -0.8\times10^{-4}\log c + 0.61\times10^{-3} \quad (7)$$

It can also be seen that the mass transfer coefficient shows higher values of mass transfer coefficient with lower values of bulk Cd^{2+} concentrations, this is attributed to the hydrogen evolution, which is the predominant cathodic reaction at low values of the inlet cadmium concentration.

In order to find the mass of Cd^{2+} deposited with time, a mass balance was conducted on three different initial concentrations of cadmium solutions (50, 200, 400 ppm). Fig. 7 illustrates the mass deposition of cadmium as a function of time. The resulted curves are also exponential with time.

3.3. Effect of electrolyte Reynolds number

Experiments were carried out to study the influence of Reynolds number of catholyte on the removal rate of Cd^{2+} from solutions with initial concentration of 200 ppm.

Fig. 8 shows the curves of normalized Cd^{2+} concentration $c(t)/c_o$ as a function of time for different catholyte Reynolds numbers (1.189, 2.377, 2.972, 3.566, 4.16). Cadmium concentration decays exponentially with time. It can be seen that higher Reynolds numbers enhance the removal of Cd^{2+}. This behavior is attributed to greater

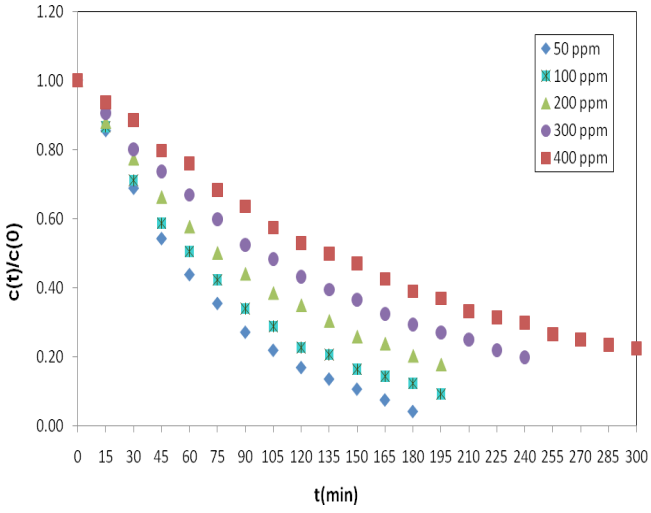

Fig. 5. Normalized concentration $c(t)/c_o$ as a function of time for removal of different Cd^{2+} concentrations and Reynolds number of 2.972.

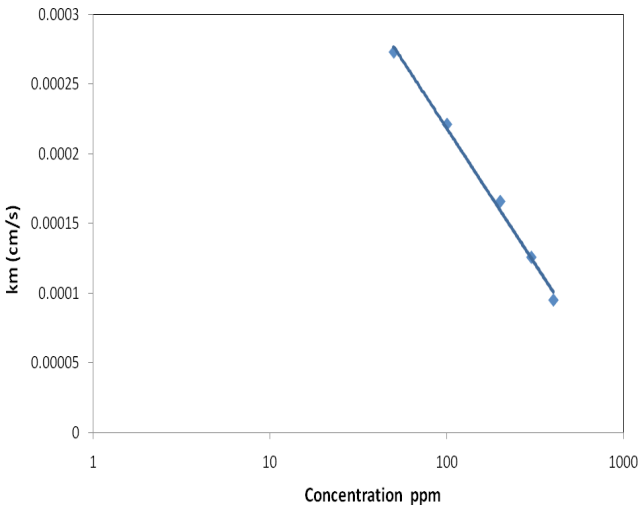

Fig. 6. Variation of mass transfer with logarithmic bulk Cd^{2+} concentrations.

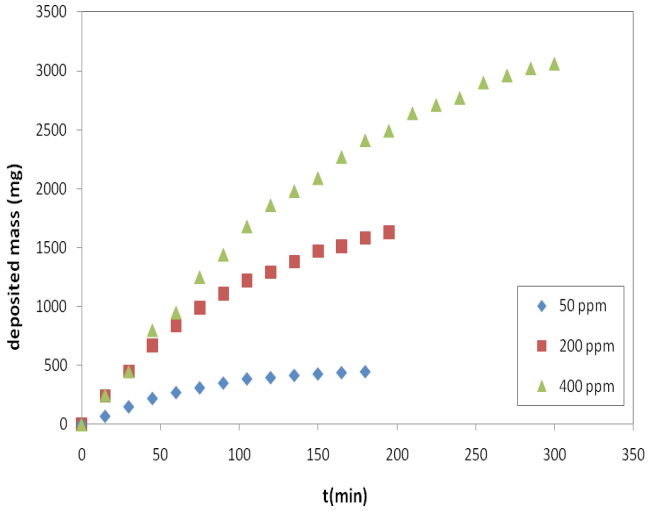

Fig. 7. Mass deposited of cadmium with time for different Cd^{2+} concentrations and Reynolds number of 2.972.

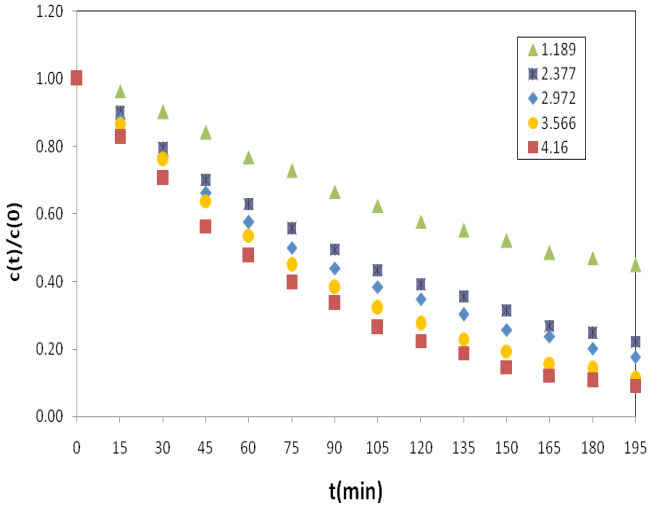

Fig. 8. Normalized concentration $c(t)/c_o$ as a function of time for Cd^{2+} removal for different Reynolds numbers and Cd^{2+} concentration of 200 ppm.

rates of mass transport of Cd^{2+} with increased electrolytes Reynolds numbers, which reduce the thickness of the boundary layer for mass transfer.

Plotting the logarithmic normalized concentration $\ln(c(t)/c_o)$ as a function of time, gives linear relationships. Following the same previous procedures, values of k_m were calculated for each Reynolds number.

In order to correlate the mass transfer coefficient with the electrolyte velocity, the estimated values of k_m were plotted (log–log) against u, giving a linear relationship. The results were correlated by the empirical expression, with CR = 0.997:

$$k_m = 0.000286u^{0.504} \quad (8)$$

3.4. Mass transfer correlations

Mass transfer coefficients estimated from the series of experiments on different Reynolds numbers were fitted to find an empirical correlation of dimensionless Sherwood number for the tubes bundle cathode under the medium and conditions of the experiments.

Starting from the typical mathematical relationship for dimensionless Sherwood number, which is suitable for electrolytic reactors design:

$$\mathrm{Sh} = m\,\mathrm{Re}^n\,\mathrm{Sc}^{1/3} \quad (9)$$

And the so called j_D factor correlation:

$$j_D = \mathrm{Sh}\,\mathrm{Re}^{-1}\,\mathrm{Sc}^{-1/3} \quad (10)$$

where m and n are empirical constants dependent on the geometry of the system [15].

The following correlation is obtained:

$$\mathrm{Sh} = 0.051\,\mathrm{Re}^{0.859}\,\mathrm{Sc}^{1/3} \quad (11)$$

for $5 < \mathrm{Re} < 20$ and Sc = 649 (calculated from rotating disc electrode experiments).

This obtained correlation is of good agreement with researchers [15].

Table 2 lists the data used for the analysis.

Figs. 9 and 10 summarize the Sherwood–Schmidt–Reynolds and j_D correlations, with CR = 0.996 and CR = 0.95, respectively.

3.5. Observations of the scanning electron microscope (SEM)

Samples of the selected used tubes were examined by the scanning electron microscope (SEM) model Hitachi S3200N, observations were made on different spots of the selected used tubes from both inner and outer surfaces.

Figs. 11 and 12 show the surface morphology of two tubes with different shaped spots of electrodeposited cadmium at a magnification of 30 μm.

Table 2
Data used for calculations of dimensionless numbers and Cd^{2+} concentration of 200 ppm

Parameters		Reynolds numbers
$10^5\,D$ ($cm^2\,s^{-1}$)	1.127	1.189
$10^2\,\nu$ ($cm^2\,s^{-1}$)	0.731	2.377
Schmidt number	649	2.972
Porosity	0.583	3.566
Equivalent diameter (d_e) (cm)	0.27	4.16

D and ν were estimated from rotating disc electrode experiments [7]

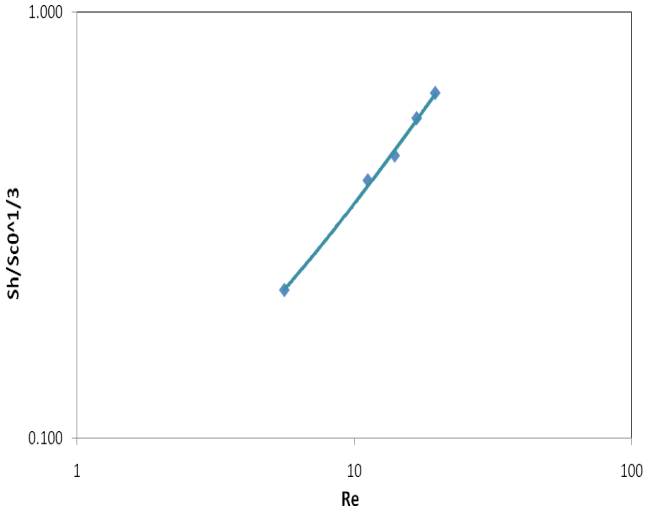

Fig. 9. Sherwood–Reynolds correlation for Cd^{2+} concentration of 200 ppm.

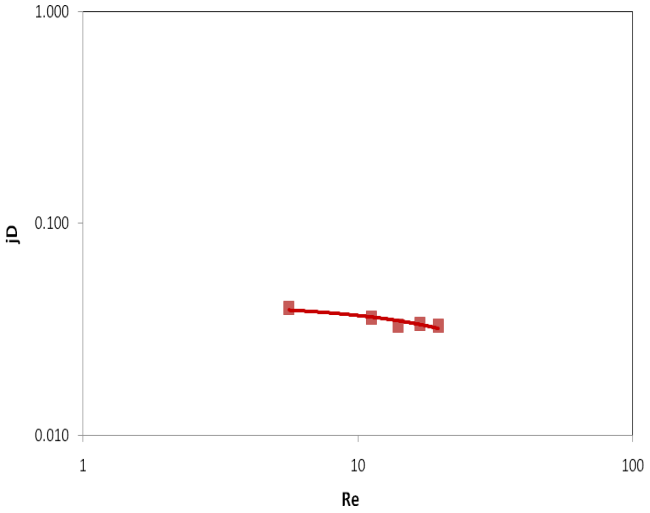

Fig. 10. j_D factor–Reynolds correlation for Cd^{2+} concentration of 200 ppm.

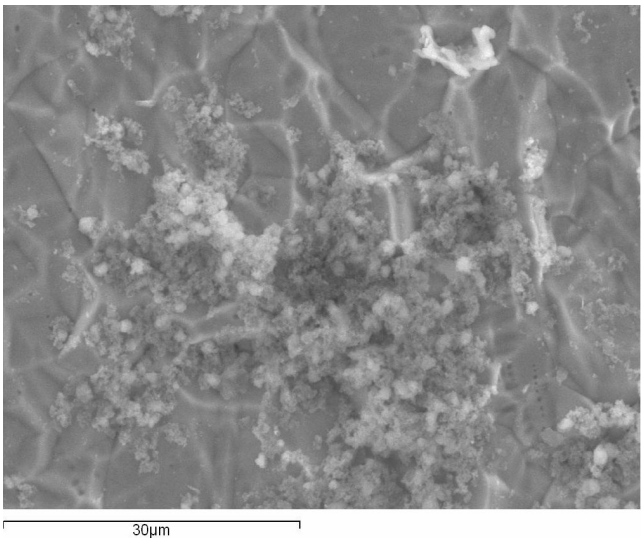

Fig. 11. Scanning electron micrograph of the first tube with electrodeposited cadmium. Magnification 30 µm.

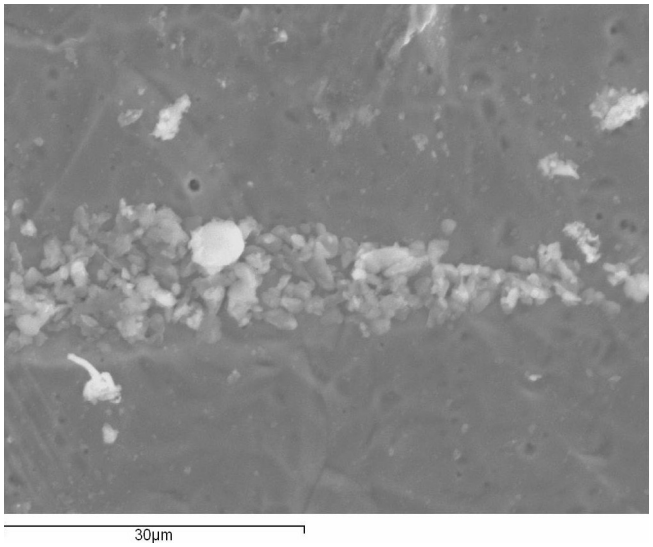

Fig. 12. Scanning electron micrograph of the second tube with electrodeposited cadmium. Magnification 30 µm.

It can be seen that cadmium is non-uniformly deposited on the tubes surfaces but it is taking the forms of scattered spots of deposits.

The images also reveal the dendritic nature of the cadmium deposits.

Fig. 13 shows the energy dispersive spectrometric (EDS) analysis, showing the presence of deposited cadmium as a peak and the qualitative/quantitative elemental analyses of the tube specimen.

The (EDS) analysis reveals the components' map of the specimen, presented as peaks. These peaks represent the constituting elements of the stainless steel tube, the electrodeposited cadmium and other deposited impurities. It can be seen that Cd has a relatively small peak compared to the other components.

The qualitative/quantitative elemental analyses of the tube specimen show that the weight % of cadmium is 0.74% in the scanned location, (some other specimen showed lower percentages), this is considered a small amount.

3.6. Deposits of cadmium powders

Analyzing the composition of the thick spongy de-

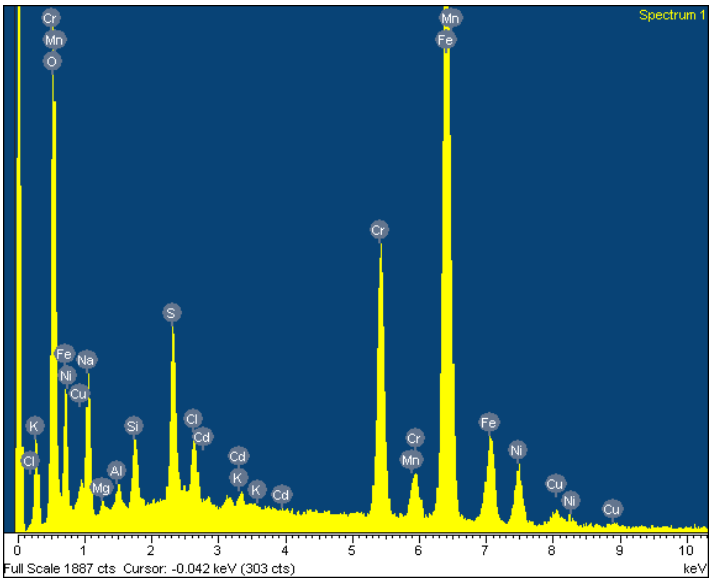

Element	Weight %	Atomic %
O K	19.69	41.64
Na K	7.08	10.42
Mg K	0.31	0.43
Al K	0.46	0.57
Si K	1.33	1.60
S K	3.62	3.82
Cl K	1.62	1.54
K K	0.21	0.19
Cr K	12.05	7.84
Fe K	45.17	27.36
Ni K	6.05	3.49
Cu K	1.68	0.90
Cd L	0.74	0.22
Total	100.00	

Fig. 15. Energy dispersive spectrometric analysis showing the presence of Cd and qualitative/quantitative elemental analyses of tube specimen.

posits contained in the catholyte samples taken from the catholyte reservoir by atomic absorption showed that it contained 150 ppm cadmium which is a relatively good amount of cadmium powders.

The formation of the deposited cadmium powders in the samples solutions and the spots of cadmium dendrites on the tubes detected by the (SEM), is depicted by the fact that cadmium electrodeposition on stationary stainless steel cathodes can take the form of trees and sprouts deposits. Earlier it was reported that neutral solutions will yield not a metallic deposit but a spongy mass on stationary cathodes, a coherent deposit may be obtained from acid solutions but the trees and sprouts are also produced in quantity [16].

The mechanism is that cadmium electrodeposition increases the cathode surface area, but after a time the deposit is detached from the cathode to the solution, then metal deposition recommences. This behavior allows removal of the cadmium as a metal powder without the need of scrapers [3].

4. Conclusions

1. The performance of the stainless steel tubes bundle electrode, operating in the batch re-circulated mode, was successful in the removal of Cd^{2+} from simulated wastewater.
2. The mass transfer coefficient increased with lower values of bulk Cd^{2+} concentration, due to hydrogen evolution; the mass transfer coefficient was correlated with the bulk concentration of Cd^{2+} in sodium sulphate by the following empirical equation, with CR = 0.995:

$$k_m = -0.8\times10^{-4}\log c + 0.61\times10^{-3}$$

3. The mass transfer coefficient increased with higher Reynolds numbers, due to the reduction in the boundary layer thickness; the mass transfer coefficient was correlated with the electrolyte velocity by the following empirical expression, with CR = 0.997:

$$k_m = 0.000268\, u^{0.504}$$

4. The overall empirical mass transfer correlation was found to be: $Sh = 0.51\, Re^{0.859}\, Sc^{1/3}$ for $5 < Re < 20$ and $Sc = 649$.
   This is in good agreement with literature.
5. The formation of deposited cadmium powders in the electrolyte samples allows the removal of cadmium as a metal powder.

Aknowledgment

We would like to express our deepest thanks and appreciations to the University of Surrey Faculty of Engineering and Physical Sciences, University of Surrey for their support to accomplish this project.

Symbols

A — Electrode surface area, m^2
A_e — Specific surface area, m^{-1}
C — Concentration, mol m^{-3}, or mg L^{-1}, or ppm
c_o — Initial concentration, mol m^{-3}, or mg L^{-1}, or ppm
c_L — Outlet concentration, mol m^{-3}, or mg L^{-1}, or ppm

$C(t)$ — Concentration at time t, mol m^{-3}, or mg L^{-1}, or ppm
CR — Correlation coefficient
D — Diffusion coefficient, m^2 s^{-1}
d_e — Equivalent diameter (a characteristic length), m
E — Electrode potential (vs. SCE), V
EC — Electrochemical cell
F — Farady constant = 96500 Coloumb, Coloumb mol^{-1}
I — Current, A
I_L — Limiting current density, A m^{-2}
i_L — Limiting current, A
j_D — Mass transfer factor
k — Decay rate constant, s^{-1}
k_m — Mass transfer coefficient, m s^{-1}
L — Electrode length, m
n — Charge number of electrode reaction
Q — Flow rate, L h^{-1}
RE — Reference electrode
Re — Reynolds number = $u_\varepsilon d_e/\nu$
SCE — Saturated calomel electrode
Sc — Schmidt number = ν/D
Sh — Sherwood number = $k_m d_e$/D
t — Time, min or s
u — Flow velocity, m s^{-1}
u_ε — Characteristic flow velocity = u/ε, m s^{-1}
V — Effective electrolyte volume (within reactor), m^3
V_e — Electrode volume, m^3
V_R — Reactor volume, m^3
V_T — Total electrolyte volume, m^3

Greek

ε — Porosity
μ — Fluid viscosity, kg m^{-1} s^{-1}
ρ — Fluid density, kg m^{-3}
ν — Kinematic viscosity, m^2 s^{-1}

References

[1] D.Simonsson, Electrochemistry for a cleaner environment, Chem. Soc. Rev., 26 (1997) 181–189.
[2] Lenntech, Water Treatment and Purification Holding BV, Heavy Metals, http://www.lenntech.com, 2009.
[3] J.M. Grau and J.M. Bisang, Removal of cadmium and production of cadmium powder using a continuous undivided electrochemical reactor with a rotating cylinder electrode, J. Chem. Technol. Biotechnol., 77 (2002) 465–472.
[4] J. Tramontina, D.S. Azambuja and M.S. Piatnicki, Removal of Cd^{2+} ions from diluted aqueous solutions by electrodeposition on reticulated vitreous carbon electrodes, J. Braz. Chem. Soc., 13 (2002) 469–473.
[5] R. Bertazzoli, C.A. Rodrigues, E.J. Dallan, M.T. Fukunaga, M.R.V. Lanza, R.R. Leme and R.C. Widner, Mass transport properties of a flow-through electrolytic reactor using a porous electrode: performance and figures of merit for Pb II removal, Braz. J. Chem. Eng., 15(4) (1998) 396–405.
[6] D. Pletcher, I. White, F.C. Walsh and J.P. Millington, Reticulated vitreous carbon cathodes for metal ion removal from process streams; Part I: Mass transport studies, J. Appl. Electrochem., 21 (1991) 659–666.
[7] T.K. Al-Shalchi, Removal of cadmium from simulated wastewaters by electrodeposition on stainless steel tubes bundle, PhD thesis, College of Engineering, University of Baghdad, 2010.
[8] J.M. Grau and J.M. Bisang, Effluent treatment using a bipolar electrochemical reactor with rotating cylinder electrodes of woven wire meshes, J. Chem. Technol. Biotechnol., 84 (2009) 1084–1089.
[9] J.M. Grau and J.M. Bisang, Electrochemical removal of cadmium from dilute aqueous solutions using a rotating cylinder electrode of wedge wire screens, J. Appl. Electrochem., 37 (2007) 275–282.
[10] G.W. Reade, P. Bond, C. Ponce de Leon and C. Walsh, The application of reticulated vitreous carbon rotating cylinder electrodes to the removal of cadmium and copper ions from solution, J. Chem. Technol. Biotechnol., 79 (2004) 946–953.
[11] A.E. Elsherief, Removal of cadmium from simulated wastewaters by electrodeposition on spiral wound steel electrode, Electrochim. Acta, 48 (2003) 2667–2673.
[12] A.J.B. Durta, A. Espinola and P.P. Borges, Cadmium removal from diluted aqueous solutions by electrowinning in a flow-by cell, Minerals Eng., 13(10–11) (2000) 1139–1148.
[13] U. Landu, Determination of laminar and turbulent mass transport rates in flow cells by the limiting current technique, AIChE Symp. Ser., 204 (1981) 75–87.
[14] A.J. Bard and L.R. Faulkner, Electrochemical Methods, Fundamentals and Applications, John Wiley and Sons, 1980.
[15] D.J. Pickett, Electrochemical Reactor Design, Elsevier, 1979.
[16] G.L. Mantell, Electrochemical Engineering, McGraw-Hill, 1960.